

双损耗 Al₂O₃基多孔吸波材料的制备及其吸波性能

乔宇爔¹ 李红伟^{1,2} 张利琪¹ 吉雪丽¹ 周亮^{1,2}

(1 长安大学材料科学与工程学院, 西安 710061)

(2 长安大学交通铺面材料教育部工程研究中心, 西安 710061)

文 摘 基于片状 Al₂O₃陶瓷互锁结构强度高的特点, 制备出夹杂石墨的高气孔率的 Al₂O₃多孔陶瓷, 并通过原位还原在多孔骨架中制备出 Ni微粒, 形成一种轻质的双损耗陶瓷基吸波材料。通过XRD、FE-SEM 和 EDS 研究了还原温度对多孔吸波材料的组成、微观形貌、元素分布和吸波性能的影响。结果表明, 还原温度升温至 700 °C 可将多孔网络中 Ni 完全还原, 形成以堆叠互锁 Al₂O₃为基, 夹杂片状石墨和孔表面覆盖 Ni微粒的双损耗轻质吸波材料。当复合材料厚度为 6.5 mm 时, 最小反射损耗为 -35.01 dB, 有效吸收带宽达到 1.75 GHz。片状 Al₂O₃锁定的石墨片构筑的导电网络, Ni微粒与基体之间的极化效应等共同促进复合材料良好的微波吸收性能。

关键词 微波吸收, 原位还原, 氧化铝, 多孔陶瓷, 镍微粒

中图分类号: TM25

DOI: 10.12044/j.issn.1007-2330.2023.05.007

Fabrication and Microwave Absorbing Performance of Porous Al₂O₃ Ceramic With Double Loss of Electromagnetic Wave

QIAO Yuxi¹ LI Hongwei^{1,2} ZHANG Liqi¹ JI Xueli¹ ZHOU Liang^{1,2}

(1 School of Materials Science and Engineering, Chang'an University, Xi'an 710061)

(2 Engineering Research Center of Transportation Materials of Ministry of Education, Chang'an University, Xi'an 710061)

Abstract Based on the high strength of flake Al₂O₃ ceramic interlocking structure, Al₂O₃ porous ceramics with high porosity and graphite were prepared, and Ni particles were prepared by in-situ reduction in the porous skeleton to form a lightweight double-loss ceramic-based absorbing material. The effects of reduction temperature on the composition, microstructure, element distribution and microwave absorption properties of porous absorbing materials were studied by XRD, FE-SEM and EDS. Results concluded the following. The results show that Ni on the framework can be completely reduced when the temperatures is up to 700 °C. The composite with a double loss function is composed of an interlocking Al₂O₃ matrix with graphite flakes embedded in it and Ni particles on the surface of pores. As the thickness of the composite is 6.5 mm, the reflection loss (RLmin) value is 35.01 dB and the effective bandwidth (RL ≤ 10 dB) is 1.75 GHz. Microwave absorption can be attributed to the conductive network formed by graphite flakes between flaky Al₂O₃ grains, as well as to the good impedance matching and polarization effect caused by the Ni particle-matrix interface.

Key words Microwave absorption, In-situ reduction, Alumina, Porous ceramics, Ni particle

0 引言

日益广泛应用的各类电子设备丰富和便利了人们的现代生活, 与此同时也造成了趋于严重的电磁污染, 对人们的身体健康和精密电子设备的安全使用产生巨大的危害^[1-4]。为了防护电磁污染, 研究人员开发各类吸波材料, 通过不同的损耗机制将吸收

的电磁波直接消耗或转化为其他形式的能量, 达到电磁衰减的目的。大量的理论和实验研究表明, 理想的吸波材料需要具备轻质、有效吸收频带宽、厚度薄且吸收强等特点^[5]。

通常地, 吸收剂是影响吸波材料性能的关键, 基于微波损耗机理可分为介电损耗和磁损耗两类。介

收稿日期: 2022-03-30

基金项目: 长安大学中央高校基础研究项目(No. 300102310110); 长安大学创新团队项目(No. 300102311403); 长安大学2020大学生创新创业训练计划项目(S202010710176X)

第一作者简介: 乔宇爔, 1994年出生, 硕士, 主要从事多孔陶瓷吸波方面的研究工作。E-mail: qiaoyuxi0607@163.com

通信作者: 李红伟, 1980年出生, 讲师, 主要从事先进材料结构设计及优化工作。E-mail: lhw@chd.edu.cn

电吸收剂中碳材料的介电性优异,且其密度低、化学稳定性良好,广泛应用于吸波材料,但是其较高的电导率易形成电磁波的反射^[6],导致阻抗失配;铁磁性金属及其氧化物是优良的磁损耗型吸收剂,但其密度高在一定程度上限制了它们的应用^[7-8]。单组分吸收剂吸收强度低、密度高等缺点往往不能满足效能要求。研究发现,介电损耗和磁损耗吸收剂协同使用可获得更加良好阻抗匹配和高效电磁衰减吸波材料,如 MWCNTs/Fe/Co/Ni^[9]、ZnO/CNWs^[10]、Fe@CNT/SiC^[11]。设计制备出轻质、吸波效能好、成本低的吸波材料仍是一项巨大的挑战。

多孔陶瓷载体具有轻质的特点,大量的孔隙可以降低陶瓷的介电常数,平衡了吸波材料与空气之间的阻抗间隙^[12-14],形成的非均匀界面导致入射电磁波的多次反射和散射;如 CNW/Si₃N₄^[15]、CNWs-SiO₂/3Al₂O₃·2SiO₂^[16]等多孔吸波材料均显示出优异的吸波性能。Al₂O₃陶瓷具有强度高、硬度高、耐高温、化学惰性大、介电损耗低等特点,在一定条件下可烧结出片状的Al₂O₃晶粒,微观上形成堆叠互锁结构,兼具高气孔率和高强度^[17];同时,片状结构有利于负载微纳米吸波剂和电磁波在孔中的反射,有望成为一种较为理想的微波吸收载体。本文将具有物理化学稳定性好、密度低、成本低、来源广泛的鳞片石墨(FG)^[18]与片状晶构成多孔Al₂O₃陶瓷复合,作为

介电吸波剂锁定在基体中,通过浸渍法调整碳热还原温度将磁性成分Ni颗粒负载于片状多孔Al₂O₃网络结构上,讨论形成的双损耗轻质复合结构对吸波性能的影响。

1 实验

1.1 样品制备

为了制备出高气孔率的Al₂O₃陶瓷支撑体,以粒径500 nm的商用α-Al₂O₃为初始原料,并加入4%(*w*)的AlF₃和10%(*w*)的TEOS,以引入F和Si元素抑制高温下Al₂O₃晶体(0001)面的生长,形成片状晶互锁的Al₂O₃陶瓷。随后添加适量的水和无水乙醇,湿混12 h,干燥并研磨得到白色粉料。将上述粉料与3%(*w*)的鳞片石墨粉(粒径40 μm)混合均匀,另加入少量PVA黏结剂模压得到24 mm×11 mm×3 mm的坯体,干燥后将坯体置于密封的刚玉坩埚中,缓慢升温至1 350 °C并保温3 h,得到多孔陶瓷,记作C/Al₂O₃。将可溶性淀粉、Ni(NO₃)₂·6H₂O和水以质量比1:10:31溶解后混合均匀形成溶液,将多孔样品置入该溶液中真空浸渗30 min,干燥后将试样在Ar和少量H₂的混合气氛下以5 °C/min分别升温至300、500和700 °C,各保温2 h,不同温度处理后的样品标记为Ni/C300、Ni/C500和Ni/C700,以备测试。制备流程示意图如图1所示。

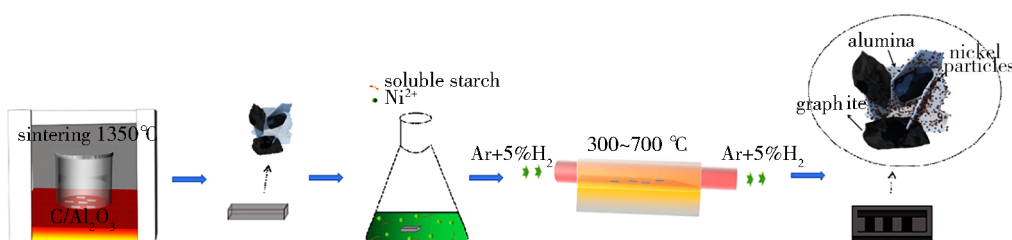


图1 双损耗型多孔Al₂O₃陶瓷的制备过程示意图

Fig. 1 Schematic illustration of preparation of porous Al₂O₃ absorbing ceramic with double loss of electromagnetic wave

1.2 表征

烧结后的各试样采用阿基米德法来测定其体积密度和气孔率;试样的物相由X射线衍射仪(D8 ADVANCE,德国,Bruker)表征,测试条件为Cu靶,入射光λ=0.154 6 nm,管电压和管电流分别为40 kV和40 mA;试样喷金后,其断口微观形貌则通过FE-SEM(S4800,日本,HITACHI)观测,测试条件为15 kV和10 mA。试样加工成矩形(22.86 mm×10.16 mm),通过矢量网络分析仪(E8362 B PNA,美国,Agilent)采用矩形波导法测量出各复合材料在X波段的复介电常数和复磁导率。根据传输线理论,计算复合涂层的反射损耗(RL)、输入阻抗(Z_{in})的公式为^[19-20]:

$$RL(\text{dB}) = 20\lg \left| \left(Z_{\text{in}} - Z_0 \right) / \left(Z_{\text{in}} + Z_0 \right) \right| \quad (1)$$

$$Z_{\text{in}} = Z_0 \sqrt{\mu_r / \epsilon_r} \tanh \left[j \left(2\pi f d / c \right) \sqrt{\mu_r \epsilon_r} \right] \quad (2)$$

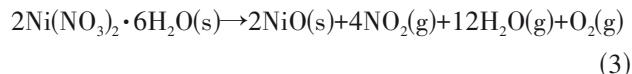
式中,Z₀为自由空间的输入阻抗,μ_r和ε_r为吸收器的相对磁导率和介电常数,f为入射波的频率,c为自由空间的光速,d为吸收器的厚度。

2 结果和讨论

2.1 双损耗多孔材料的形貌和相组成

图2为片状C/Al₂O₃基体和不同温度还原后的Ni/C复合材料的XRD图。通过1 350 °C密封条件下的高温烧结,烧成的样品主要成分为α-Al₂O₃(PDF#99-0036)和石墨(PDF#41-1487)。浸渍含镍的溶液后,当还原温度为300 °C时,在2θ为37.3°、43.3°、62.8°

等处出现的衍射峰表明,形成了NiO(PDF#47-1049)。这归因于硝酸镍的分解,其分解的过程为^[21]:



当还原温度升高至500 °C,则出现了44.3°,51.7°和76.2°的衍射峰,其对应于Ni单质(PDF#04-0850)的峰。表明500 °C可将部分NiO和来自于淀粉裂解的残余C发生碳热还原形成Ni;还原温度升高到700 °C,NiO的衍射峰完全消失,Ni峰增强,表明此时NiO被完全还原为Ni,相关反应为^[22]:

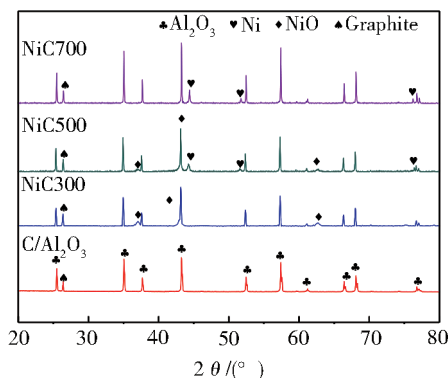
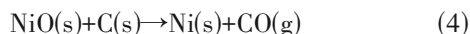
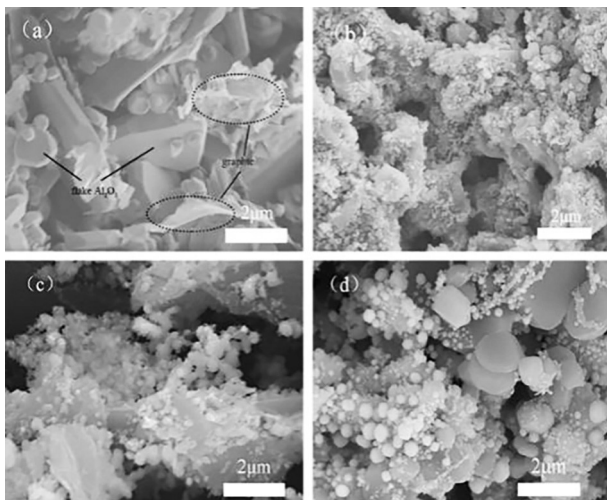


图2 C/Al₂O₃和在不同温度还原后Ni/C复合材料的XRD
Fig. 2 XRD patterns of C/Al₂O₃ and Ni/C composites prepared at different reduction temperature

图3为C/Al₂O₃基体和不同温度还原后复合材料的断口微观形貌。



注:(a)C/Al₂O₃;(b)Ni/C300;(c)Ni/C500;(d)Ni/C700。
图3 C/Al₂O₃和不同温度还原后Ni/C复合材料的断口SEM图

Fig. 3 SEM images of the fracture of C/Al₂O₃ and Ni/C composites prepared at different reduction temperature

其中图3(a)显示了混有石墨的片状C/Al₂O₃基体形貌,基体中Al₂O₃呈现六角形的片状,较大晶粒的Al₂O₃堆叠互锁,石墨片被嵌于片状Al₂O₃间。不同温度还原

Ni后的复合材料如图3(b)-(d)所示。图3(b)和图3(c)中,近纳米级颗粒覆盖了片状Al₂O₃晶粒表面,分布在Al₂O₃形成的孔隙表面。升高了还原温度,球状颗粒尺寸增加。结合XRD分析,还原温度较低时,仅裂解得到极细小的NiO颗粒;随着还原温度的升高,部分NiO还原成细小的Ni颗粒;当温度提高到700 °C时,能够将Ni全部还原,但较高的温度使得Ni球状颗粒长大较快,甚至接近1 μm。表1中列出了Ni/C复合材料的气孔率和体积密度,并与其他材质多孔吸波材料进行对比^[23-25]。值得注意的是,碳热还原处理后样品密度降低而开气孔率显著提高。

表1 轻质吸波陶瓷材料的密度和开气孔率

Tab. 1 Densities and porosities of lightweight microwave absorbing ceramics

种类	气孔率/%	体积密度/g·cm ⁻³	参考文献
Sc ₂ Si ₂ O ₇	33.00	2.10	[23]
Si ₃ N ₄	40.00	1.97	[24]
SiCN-Si ₃ N ₄	43.05	—	[25]
C/Al ₂ O ₃	45.54 ± 1.62	2.07 ± 0.16	本工作
Ni/C300	48.01 ± 1.56	1.97 ± 0.04	本工作
Ni/C500	53.85 ± 3.76	1.77 ± 0.21	本工作
Ni/C700	58.38 ± 1.10	1.50 ± 0.16	本工作

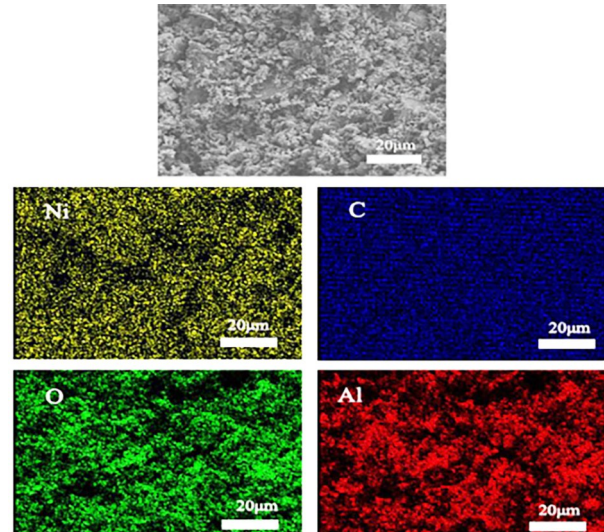


图4 Ni/C700复合材料的EDS元素分布图
Fig. 4 EDS elemental mapping images of Ni/C700 composite

为了分析浸渍还原形成的双损耗轻质材料的元素分布特征,对Ni/C700复合材料的EDS分析如图4所示。O和Al在Ni/C700复合材料中的元素分布高度一致,因其共同来自于Al₂O₃晶体。Ni元素的分布较为均匀,主要沿着片状Al₂O₃分散,与C元素分布却不相似,表明浸渍沉积原位还原的Ni吸收剂附着在基体上且分布均匀,同时掺杂的石墨吸收剂可以在

烧结制备中得到保留；石墨网络可以为电子的传输提供导电路径，有利于高导电损耗；细小的Ni颗粒则由于大量的界面形成较优的磁损耗。分两步制备双吸收剂的策略，则有利于吸波性能的调控优化。

2.2 电磁性能

介电常数实部(ϵ')和虚部(ϵ'')分别代表材料对电磁波的储存容量和损耗能力^[26-27]。如图5所示，片状C/Al₂O₃基体拥有较高的介电常数实部和虚部。随着还原温度从300 °C升高至700 °C，Ni/C复合材料的实部和虚部的平均值分别从3.63和0.42升高至8.53和1.01。复介电常数的变化取决于它们的介电损耗机制不同。介电损耗主要分为电导损耗和极化损耗，极化损耗又进一步可以分离为偶极取向极化和界面极化^[28]。C/Al₂O₃基体内片状石墨之间及片状

石墨与基体间形成连续的导电网络，电子迁移会导致强烈的电导损耗^[29]。另一方面，界面增加使自由电荷在界面处大量聚集，在交变电场下形成的电子弛豫极化和界面极化增强。对于Ni/C复合材料，还原后的Ni和NiO均匀沉积在堆叠互锁的片状Al₂O₃上，片状结构增加了相互连接的可能性，促使更多导电网络的形成，但部分片状石墨在还原过程中可能被损耗，碳的导电网络和电子传输被削弱。复介电常数虚部主要与电导率(σ)和极化弛豫损耗($\epsilon''_{\text{relax}}$)相关，根据德拜理论可知^[30]：

$$\epsilon'' = \epsilon''_{\text{relax}} + \frac{\sigma}{2\pi\epsilon_0} \quad (5)$$

随着还原温度的升高，Ni的晶型更为完整。因此，在Ni/C500和Ni/C700内部产生了大量缺陷作为偶极子中心，极化弛豫损耗会使介电常数虚部增加^[31-32]。

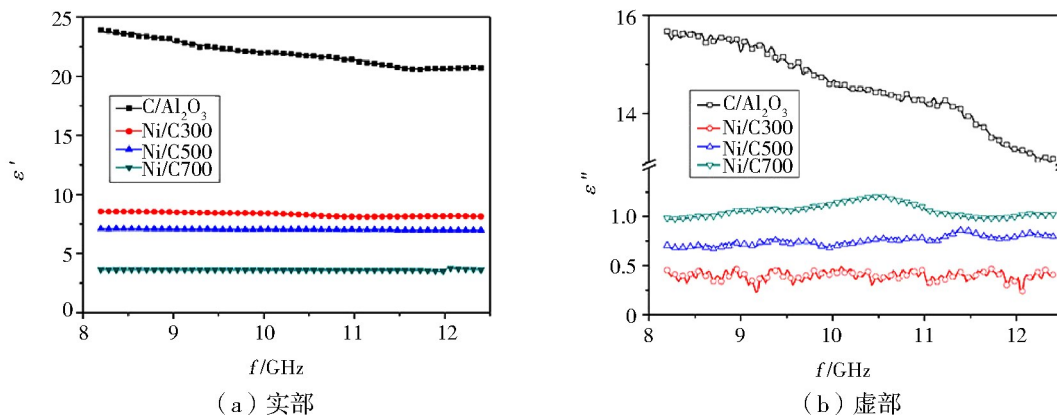


图5 C/Al₂O₃和不同温度还原后Ni/C复合材料的复介电常数

Fig. 5 Complex permittivity of C/Al₂O₃ and Ni/C composites reduced at different temperature

图6为不同温度还原后的Ni/C复合材料的复磁导率的实部(μ')和虚部(μ'')。由图6(a)可知，Ni/C复合材料的实部(μ')随频率的增加而下降。此外，在 μ'' 曲线上还存在共振峰，普遍认为磁损耗主要来源于自然

共振、交换共振、涡流损耗、磁滞损耗及畴壁位移^[33-34]。由于外加磁场较弱，磁滞损耗可以被排除，而畴壁共振通常发生在1~100 MHz内^[35]，因此这主要是由还原形成的Ni磁性颗粒的自然共振和交换共振引起的。

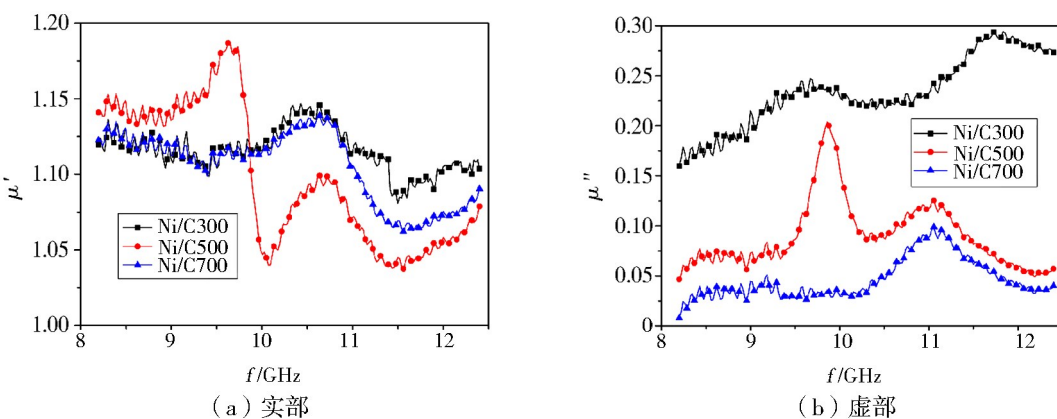


图6 不同温度还原后Ni/C复合材料的复磁导率

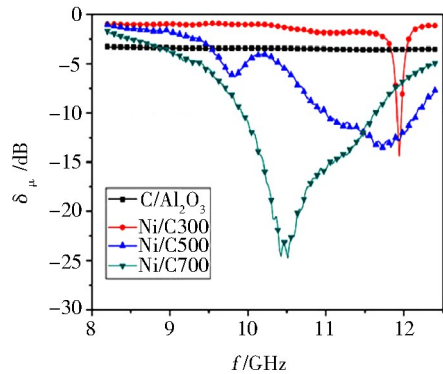
Fig. 6 The complex permeability of Ni/C composites reduced at different temperature

整体而言,Ni/C复合材料的低复磁导率可能与沉积量较少相关,特别是复合材料的孔隙率及孔径大小都会直接影响Ni颗粒的沉积。因此,本文中Ni/C双负载多孔C/Al₂O₃复合材料的微波吸收机制主要依赖于电导损耗,它们的复磁导率变化范围比较小。

2.3 微波吸收性能

根据线传输理论,通过计算反射损耗评估复合材料在8.2~12.4 GHz频带内的微波吸收性能,如图7(a)所示。当还原温度为700 °C时,其吸波性能最佳,在10.57 GHz频率处获得最小反射损耗-22.68 dB,有效吸收频带宽为1.68 GHz(9.94~11.62 GHz)。

Ni/C700复合材料厚度变化的反射损耗如图7

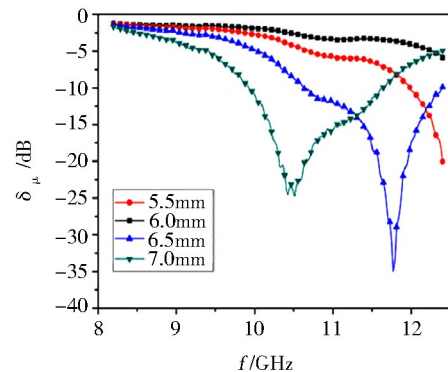


(a) 在不同温度下还原(7 mm)反射损耗

(b)所示,当样品厚度为6.5 mm时,Ni/C700复合材料在11.77 GHz时具有最小的反射损耗-35.01 dB,在8.2~12.4 GHz频率范围内的有效吸收频带宽为1.75 GHz。明显地,随着样品厚度的增加,Ni/C700的RL峰逐渐向低频移动。该现象可以用λ/4理论来解释,它描述了匹配频率(f_m)和厚度(d_m)之间的关系,可用以下公式表示^[36]:

$$f_m = \frac{c}{4d_m} \times \frac{1}{\sqrt{\epsilon' \mu'}} \left(1 + \frac{\tan^2 \delta_\mu}{8} \right)^{-1} \quad (6)$$

式中,c代表光速,δ_μ代表磁损耗正切。由公式可知,匹配频率(f_m)和厚度(d_m)及 $\sqrt{\epsilon' \mu'}$ 成反比。



(b) 不同厚度的反射损耗(700 °C)

图7 C/Al₂O₃和复合材料的反射损耗

Fig. 7 C/Al₂O₃ and composite materials

3 结论

(1)在1350°C密封环境下可烧结出片状Al₂O₃晶粒互锁且夹杂石墨片的多孔陶瓷,浸渍淀粉和硝酸镍的溶液后可在700 °C将Ni颗粒完全碳热还原,负载于多孔网络中,该复合吸波材料密度为1.50 g/cm³,开气孔率达到58.38%。

(2)含有Ni颗粒和石墨片的双损耗多孔材料厚度为6.5 mm时,其最小反射损耗为-35.01 dB,有效带宽为1.75 GHz,显示出较为良好的X波段微波吸收性能。

(3)Ni颗粒和锁定于片状Al₂O₃之间的石墨片形成复合吸收剂,石墨片构筑的导电网络,镍颗粒与基体之间的极化效应共同促进复合材料良好的微波吸收性能。

参考文献

[1] CHEN Z P, XU C, MA C Q, et al. Lightweight and flexible graphene foam composites for high-performance electromagnetic interference shielding[J]. Advanced Materials, 2013, 25(9):1296-1300.

[2] HUANG X G, ZHANG J, LAI M, et al. Preparation and microwave absorption mechanisms of the NiZn ferrite nanofibers[J]. Journal of Alloys and Compounds, 2015, 627:367-373.

[3] LIU Y, SU X L, LUO F, et al. Enhanced electromagnetic and microwave absorption properties of carbonyl iron/Ti₃SiC₂/epoxy

resin coating [J]. Journal of Materials Science Materials in Electronics, 2017, 29(3):2500-2508.

[4] FENG Y B, QIU T, SHEN C Y, et al. Electromagnetic and absorption properties of carbonyl iron/rubber radar absorbing materials [J]. IEEE Transactions on Magnetics, 2006, 42(3):363-368.

[5] LI G M, WANG L C, LI W X, et al. NiFe₂O₄, Fe₃O₄-Fe_xNi_y or Fe_xNi_y loaded porous activated carbon balls as lightweight microwave absorbent[J]. Rsc. Advances, 2014, 5(11):8248-8257.

[6] CUI J, ZHOU Z H, JIA M Y, et al. Solid polymer electrolytes with flexible framework of SiO₂ nanofibers for highly safe solid lithium batteries[J]. Polymers, 2020, 12(6):1324-1335.

[7] KUMAR A, AGARWALA V, SINGH D, et al. Effect of milling on dielectric and microwave absorption properties of SiC based composites[J]. Ceramics International, 2014, 40(1):1797-1806.

[8] LIU Y, LI Y Y, LUO F, et al. Mechanical, dielectric and microwave absorption properties of TiC/cordierite composite ceramics [J]. Journal of Materials Science Materials in Electronics, 2017, 28(16):12115-12121.

[9] WEN F S, ZHANG F, LIU Z Y, et al. Investigation on microwave absorption properties for multiwalled carbon nanotubes/Fe/Co/Ni nanopowders as lightweight absorbers[J]. The Journal of Physical Chemistry C, 2011, 115(29):14025-14030.

- [10] KONG L, YIN X W, HAN M K, et al. Carbon nanotubes modified with ZnO nanoparticles: High-efficiency electromagnetic wave absorption at high-temperatures [J]. Ceramics International, 2015, 41(3):4906–4915.
- [11] MEI H, ZHAO X, GUI X C, et al. SiC encapsulated Fe@CNT ultra-high absorptive shielding material for high temperature resistant EMI shielding [J]. Ceramics International, 2019, 45(14):17144–17151.
- [12] LIU P, GAO S, WANG Y, et al. Metal-organic polymer coordination materials derived Co/N-doped porous carbon composites for frequency-selective microwave absorption [J]. Composites Part B Engineering, 2020, 202(1):108406.
- [13] ZHAO H, SEOW J, CHENG Y, et al. Green synthesis of hierarchically porous carbons with tunable dielectric response for microwave absorption [J]. Ceramics International, 2020, 46(10):15447–15455.
- [14] ZHOU X F, JIA Z R, ZHANG X X, et al. Controllable synthesis of Ni/NiO@ carbon hybrid composites towards remarkable electromagnetic wave absorption and wide absorption bandwidth [J]. Journal of Materials Science & Technology, 2021, 87:120–132.
- [15] SUN C, GUO Y, XU X, et al. In situ preparation of carbon/Fe₃C composite nanofibers with excellent electromagnetic wave absorption properties [J]. Composites Part A: Applied Science and Manufacturing, 2017, 92:33–41.
- [16] DONG Y, FAN X, WEI H, et al. A lightweight CNWs-SiO₂/3Al₂O₃·2SiO₂ porous ceramic with excellent microwave absorption and thermal insulation properties [J]. Ceramics International, 2020, 46(12):20395–20403.
- [17] HONDA S, HASHIMOTO S, ITO Y, et al. Improvement on characteristics of porous alumina from platelets using a TEOS treatment [J]. Ceramics International, 2013, 39(2):1265–1270.
- [18] FAN Y, YANG H, LI M, et al. Evaluation of the microwave absorption property of flake graphite [J]. Materials Chemistry & Physics, 2009, 115(2/3): 696–698.
- [19] GAO Z, XU B, MA M, et al. Electrostatic self-assembly synthesis of ZnFe₂O₄ quantum dots (ZnFe₂O₄@C) and electromagnetic microwave absorption [J]. Composites, 2019, 179(15):107417. 1–107417. 11.
- [20] WANG J H, TAN J, OR S W. Enhanced microwave electromagnetic properties of core/shell/shell-structured Ni/SiO₂/ polyaniline hexagonal nanoflake composites with preferred magnetization and polarization orientations [J]. Materials & Design, 2018, 153(5):190–202.
- [21] YUVARAJ S, FAN-YUAN L, TSONG-HUEI C, et al. Thermal decomposition of metal nitrates in air and hydrogen environments [J]. Journal of Physical Chemistry B, 2003, 107(4):1044–1047.
- [22] JAGTAP S B, KALE B, GOKARN A N. Carbothermic reduction of nickel oxide: Effect of catalysis on kinetics [J]. Metallurgical Transactions B, 1992, 23(1):93–96.
- [23] WEI H, YIN X, HOU Z, et al. A Novel SiC-based microwave absorption ceramic with Sc₂Si₂O₇ as transparent matrix [J]. Journal of the European Ceramic Society, 2018, 38(12):4189–4197.
- [24] PAN H, YIN X, XUE J, et al. The microstructures, growth mechanisms and properties of carbon nanowires and nanotubes fabricated at different CVD temperatures [J]. Diamond & Related Materials, 2017, 72:77–86.
- [25] LIU X F, ZHANG L T, YIN X W, et al. The microstructure of SiCN ceramics and their excellent electromagnetic wave absorbing properties [J]. Ceramics International, 2015, 41(9):11372–11378.
- [26] DENG Z, LI Y, ZHANG H B, et al. Lightweight Fe@C hollow microspheres with tunable cavity for broadband microwave absorption [J]. Composites, 2019, 177(15):107346. 1–107346. 8.
- [27] GOLCHINVAFA S, MASOUDPANAH S M, JAZIREHPOUR M, et al. Magnetic and microwave absorption properties of FeCo/CoFe₂O₄ composite powders—science direct [J]. Journal of Alloys and Compounds, 2019, 809(15):151746–151746.
- [28] REN F, YU H, WANG L, et al. Current progress on the modification of carbon nanotubes and their application in electromagnetic wave absorption [J]. RSC Advances, 2014, 4(28):14419.
- [29] YANG Q, SHI Y, FANG Y, et al. Construction of polyaniline aligned on magnetic functionalized biomass carbon giving excellent microwave absorption properties [J]. Composites Science and Technology, 2019, 174(12):176–183.
- [30] QING Y, XUAN W, ZHOU Y, et al. Enhanced microwave absorption of multi-walled carbon nanotubes/epoxy composites incorporated with ceramic particles [J]. Composites Science and Technology, 2014, 102(4):161–168.
- [31] WANG F Y, SUN Y Q, LI D R, et al. Microwave absorption properties of 3D cross-linked Fe/C porous nanofibers prepared by electrospinning [J]. Carbon, 2018, 134(20):264–273.
- [32] LI D R, GUO K, WANG F Y, et al. Enhanced microwave absorption properties in C band of Ni/C porous nanofibers prepared by electrospinning [J]. Journal of Alloys and Compounds, 2019, 800:294–304.
- [33] ZHANG K, GAO X, ZHANG Q, et al. Preparation and microwave absorption properties of asphalt carbon coated reduced graphene oxide/magnetic CoFe₂O₄ hollow particles modified multi-wall carbon nanotube composites [J]. Journal of Alloys and Compounds, 2017, 723:912–921.
- [34] XIE Z G, GENG D Y, LIU X G, et al. Magnetic and microwave-absorption properties of graphite-coated (Fe, Ni) nanocapsules [J]. Journal of Materials Science & Technology, 2011, 7(27):607–614.
- [35] LI G, WANG L, LI W, et al. Fe⁺, Co⁺, and Ni⁺ loaded porous activated carbon balls as lightweight microwave absorbents [J]. Chemphyschem A European Journal of Chemical Physics & Physical Chemistry, 2016, 6(16):3458–3467.
- [36] SUN J, XU H L, SHEN Y, et al. Enhanced microwave absorption properties of the milled flake-shaped FeSiAl/graphite composite [J]. Journal of Alloys & Compounds, 2013, 548(8):18–22.